Punjab University
Journal of Mathematics (ISSN 1016-2526)
Vol. 50(3)(2018) pp. 101-113

Global Image Segmentation Model of Inhomogeneous Noisy Type Images Using Increasing Natural Logarithmic Function

Sartaj Ali
Department of Mathematics,
Karnal Sher Khan Cadet College Swabi, Pakistan.
Email: sartajbs2@gmail.com

Beenesh Dayyan
Department of Mathematics,
University of Peshawar, Pakistan.
Email: beeneshdayyan@yahoo.com

Received: 23 June, 2017 / Accepted: 16 January, 2018 / Published online: 13 April, 2018

Abstract. This manuscript focuses on new image segmentation model for noisy and intensity inhomogeneity images on the basis of natural logarithmic increasing density function. Local image information is necessary for inhomogeneous images, but it is ineffective for noisy images. As a result local information misguides the motion of active contour. However, the natural logarithmic function in new proposed model is capable to capture minute details of images. Moreover, it also reduces the noise in the images and helps to clarify the exact boundaries. Comparing with local Chan-Vese Model, our new proposed model gives better performance while treating noisy and intensity inhomogeneity images. Experiments on noisy and intensity inhomogeneity images show the robustness of our new proposed model.

AMS (MOS) Subject Classification Codes: A4230V, B6135, C1250M, C5260B
Key Words: Image Segmentation, Level Set, Statistical Model, Gaussian Distribution.

1. Introduction

The segmentation of image is one of the difficult tasks in the field of image processing and computer vision. However, segmentation of image is employed vastly in engineering sciences and medical sciences. Its objective is to divide an image in different parts to make it meaningful and easier to analyze, so for detail study see monographs such as [2, 4, 8, 10, 14, 15, 16, 20, 22, 24]. Many kinds of algorithm have been suggested to find the image segmentation problems till the recent times. Moreover, several approaches are used to enhance the outcome of image segmentation algorithm. Among these, LCV model is of great importance, and it is used both for local and global image information in the process image of segmenting. While performing few iterations in the LCV model which captures local image details to segment the images with intensity inhomogeneity more efficiently; however, the LCV model is in effective in the segmentation of noisy images. Furthermore, the re-initialization step vastly used in traditional level set approaches which is quite time consuming, and it can be abandoned by the introduction of a newly penalizing energy in term of regularization form. Due to newly penalizing energy function, the consumption of time is reduced. In addition, Level set evolution procedure having the evolution curve which automatically ends on exact boundaries/edges of the given objects. At the same time, it is also quite important to deal with the problem of segmentation in noisy images because noisy images are mostly found in medical images and satellite. For details study [1, 3, 5, 9, 12, 13, 17, 18, 21, 23, 25, 26] and references therein.

The above mentioned details encourage us to introduced a new noisy image segmentation model. The new proposed model can provide better and more efficient results when the model is applied on noisy images. This new proposed model can capture more information regarding the given noisy image; moreover, it also avoids the noise at the same time in the final segmented result. Moreover, the time-consuming re-initialization step widely adopted in traditional level set methods can be avoided by introducing a new penalizing energy to the regularization term. As a result, the time-consumption is greatly decreased. Specially, the evolving curve in level set evolution process can automatically stop on true boundaries of objects. On the other hand, traditional models can segment noisy image, but simultaneously these models also capture the noise which is defective having faulty result. For detail study of traditional image segmentation models having different approaches see the monographs such as [6, 10, 11, 12, 19, 22]. The idea of our new proposed model is the combination of the local Chan-Vese model and non-linear diffusion model which are based on noisy image segmentation. The new model considers information about the region sufficiently. It is not necessary to consider the re-initialization of the curve, due to the application of Gaussian density function, and it must be noise robust. Due to which we consider the mean as well as global variance of the given image. Compared with classical LCV model, our new model for noisy image segmentation is much better because it reduces the noise in the final segmented image. The above mentioned preference of our new model can be seen through experimental results which will be presented in the last section of this monograph.

2. Notations and Preliminaries

In this section, we discuss some previous works regarding noisy image segmentation and intensity inhomogeneity image segmentation. In more precise way, we can briefly analyze two models, which are the following:

- Nonlinear diffusion equation model for noisy image segmentation.
- Local Chen-Vese (LCV) model.

Taking in account, the main ideas and limitations regarding above mentioned models, we propose our new model in section 3 which covers some limitations of LCV model, i.e. as we know that LCV model is not capable of giving efficient and good result in noisy intensity inhomogeneity images but our propose model is better in such type of image segmentations. The robustness of our new proposed model are shown through some experimental results, in section 4 of this monograph. The last section of this monograph is devoted to the concluding note about our new Segmentation model.

Noisy Image Segmentation Based on Nonlinear Diffusion Equation (NSDB) Model. The NSDB model [7] used statistical information in order to reduce the noise in segmentation. In NSBD model the infimum variance term in FEI model is replaced by a statistical term, which is being consider as a part regarding external energy at first.

Generally the above model is given as: $\arg(min_C E(C))$, where $E(C)$ is the energy functional of this model, which has the following form:

$$E(C) = \underbrace{\alpha \oint_C g(C(s))ds}_{E_{GAC}(C)} - \underbrace{\beta \oint_c |\langle \nabla I, N \rangle| ds}_{E_{AR}(C)}$$
$$+ \underbrace{\gamma \Big[\int_{inside(C)} (-logP_1(I))ds + \int_{outside(C)} (-logP_2(I))ds \Big]}_{E_{stat}(C)}.$$

In above energy term, $I(u,v)$ represents a gray level image, $\nabla I(u,v) = \{I_u, I_v\}$ denotes the gradient vector of the given image. The notation $C : [0, L] \longmapsto R^2$ is used for a parametric curve, and α, β, γ are any positive constants. Let us consider $C(s) = \{u(s), v(s)\}$, where s denotes arc length parameter. The notation $C_s = \{u_s, v_s\}$ used for tangent vector of a curve, implies that the associated normal direction is given as $N(s) = \{-v_s, u_s\}$. The model in discussion, i.e. NSDB model, consolidate many geometric measures to a unified variational framework and obtain the required statistical active contour model. In the Gaussian density case, we have two parameter's only, i.e. mean m and variance σ^2 should be obtained. Let us consider

$$p(m,\sigma) = \frac{1}{\sqrt{2\pi\sigma}} exp(-\frac{(I(u,v) - m)^2}{2\sigma^2}),$$

then the statistical active contour model is rearranged as below:

$$\begin{cases} \phi_t = \dfrac{\partial \phi}{\partial t} = \alpha.div(g(u,v)\nabla\phi) - \beta.sign(\langle \nabla I, \nabla\phi \rangle \nabla I) + \gamma \Big[log\dfrac{\sigma_2^2}{\sigma_1^2} \\ - \dfrac{(I(u,v) - m_1)^2}{\sigma_1^2} + \dfrac{(I(u,v) - m_2)^2}{\sigma_2^2} \Big] + \lambda.div\Big[\Big(1 - \dfrac{1}{|\nabla\phi|}\Big)\Big], \end{cases}$$

where,

$$m_1(\phi) = \frac{\int_\Omega I(u,v)\chi_i(\phi)dudv}{\int_\Omega \chi_i(\phi)dudv}, \quad \sigma_i^2(\phi) = \frac{\int_\Omega (I(u,v) - m_i)^2 \chi_i(\phi)dudv}{\int_\Omega \chi_i(\phi)dudv},$$

$$\chi_1(\phi) = \mathcal{H}(\phi), \quad \chi_2(\phi) = 1 - \mathcal{H}(\phi) \quad \text{and}$$

$$\mathcal{H}(p) = \begin{cases} 1, \text{ if } p > 0 \\ 0, \text{ if } p < 0 \end{cases}$$

is a Heaviside function.

Local Chan-Vese (LCV) Model. Many traditional segmentation model faces the problem of inhomogeneity segmentation, which happen in many real world images. To overcome the problem of inhomogeneous intensity segmentation, the LCV model combine both the local and global statistical information. The general form of overall energy functional of LCV model is:

$$F = \alpha F^G + \beta F^L + F^R,$$

where F^G, F^L and F^R are global, local and regularized terms respectively and defined as:

$$F^G(\mathrm{m}_1, \mathrm{m}_2, C) = \int_{inside(C)} |I - \mathrm{m}_1|^2 dudv + \int_{outside(C)} |I - \mathrm{m}_2|^2 dudv,$$

$$F^L(\mathrm{n}_1, \mathrm{n}_2, C) = \int_{inside(C)} |I' - \mathrm{n}_1|^2 dudv + \int_{outside(C)} |I' - \mathrm{n}_2|^2 dudv,$$

and

$$F^R = \oint_C dp,$$

where C is a closed curve. m_1, m_2, n_1 and n_2 are constants inside and out side C and I' is a smooth image define as $I' = g_k * I - I$ and g_k is an average operator with $\mathrm{k} \times \mathrm{k}$ convolution size window. Now the overall energy functional of LCV model in regularized form can be formulated as:

$$\begin{aligned} F_\varepsilon(\phi, \mathrm{m}_1, \mathrm{m}_2, \mathrm{n}_1, \mathrm{n}_2) &= \mu \int_\Omega \delta_\varepsilon |\nabla\phi| dudv + \int_\Omega \frac{1}{2}(|\nabla\phi| -1)^2 dudv \\ &+ \lambda_1 \int_\Omega (I - \mathrm{m}_1)^2 \mathcal{H}_\varepsilon dudv + \lambda_1 \int_\Omega (I - \mathrm{m}_2)^2 (1 - \mathcal{H}_\varepsilon) dudv \\ &+ \lambda_2 \int_\Omega (I' - d_1)^2 \mathcal{H}_\varepsilon dudv + \lambda_2 \int_\Omega (I' - d_2)^2 (1 - \mathcal{H}_\varepsilon) dudv. \end{aligned}$$

The initial term reveal the regularized term, which is used for smoothing purpose of contour and also this term is used to make the contour tight. While the next two terms in above equation represents the local and global terms, which came in application for capturing local and global-information regarding the given image. Minimization of $F_\varepsilon(\phi, \mathrm{m}_1, \mathrm{m}_2, \mathrm{n}_1, \mathrm{n}_2)$ with respect to m_1, m_2, n_1 and n_2 yields the following:

$$\mathrm{m}_1(\phi) = \frac{\int_\Omega I \mathcal{H}_\varepsilon(\phi(u,v)) dudv}{\int_\Omega \mathcal{H}_\varepsilon(\phi(u,v)) dudv}, \qquad \mathrm{m}_2(\phi) = \frac{\int_\Omega I (1 - \mathcal{H}_\varepsilon(\phi(u,v))) dudv}{\int_\Omega (1 - \mathcal{H}_\varepsilon(\phi(u,v))) dudv},$$

$$\mathrm{n}_1(\phi) = \frac{\int_\Omega I' \mathcal{H}_\varepsilon(\phi(u,v)) dudv}{\int_\Omega \mathcal{H}_\varepsilon(\phi(u,v)) dudv}, \qquad \mathrm{n}_2(\phi) = \frac{\int_\Omega I' (1 - \mathcal{H}_\varepsilon(\phi(u,v))) dudv}{\int_\Omega (1 - \mathcal{H}_\varepsilon(\phi(u,v))) dudv}.$$

By minimizing F_ε with respect to ϕ, the Euler-Lagrange's equation for ϕ is given by:

$$\begin{cases} \delta_\varepsilon \Big[\mu \mathrm{div}\Big(\frac{\nabla\phi}{|\nabla\phi|}\Big) + \lambda_1 \Big(- (I - \mathrm{m}_1)^2 + (I - \mathrm{m}_2)^2 \Big) & \\ +\lambda_2 \Big(- (I' - \mathrm{n}_1)^2 + (I' - \mathrm{n}_2)^2 \Big) \Big] = 0 & \text{in } \Omega, \\ \frac{\partial\phi}{\partial\vec{n}} = 0 & \text{on } \partial\Omega. \end{cases}$$

The below equation is consider for solution.

$$\begin{cases} \phi_t = \dfrac{\partial \phi}{\partial t} = \delta_\varepsilon \Big[\lambda_1 \Big(-(I-\mathrm{m}_1)^2 + (I-\mathrm{m}_2)^2\Big) + \lambda_2 \Big(-(I'-\mathrm{n}_1)^2 + (I'-\mathrm{n}_2)^2\Big)\Big] \\ + \Big[\mu\delta_\varepsilon \nabla.\Big(\dfrac{\nabla\phi}{|\nabla\phi|}\Big) + \Big(\nabla^2\phi - \nabla.\dfrac{\nabla\phi}{|\nabla\phi|}\Big)\Big], \qquad \text{in } \Omega, \\ \phi(u,v,t) = \phi_0(u,v,0), \qquad \text{in } \Omega. \end{cases}$$

Thus LCV model encompass the inhomogeneity problems. In fact, LCV model has also some drawbacks, because it fails in images which has low contrast, images regarding low frequencies, unilluminated objects, overlapping regions of homogeneous intensities, in such situations the results of the LCV model is not to much satisfactory.

3. Proposed Local Chan-Vese Noisy Image Segmentation Model:

This section deals with the study of our new proposed SEGMENTATION model. It is known that LCV model perform better in intensity inhomogeneity images but fails in noisy image segmentation. Since, LCV model uses local image information due to which it sometimes almost fails to segment some sort of noisy images. Hence, to reduce that mention limitations regarding LCV model, we proposed a new model in the following way:

For our new proposed model, we define a new logarithmic density function and also use few statistical information to reduce the problem regarding image segmentation in such type of noisy images. The energy functional of our new proposed model is given by:

$$\begin{aligned} \mathcal{Q}(\zeta_1, \zeta_2, \chi_1, \chi_2, \varsigma_1^2, \varsigma_2^2, \varsigma_3^2, \varsigma_4^2, \psi) &= \xi_1\xi_2 \int_{inside(\Gamma)} (\ln \pounds_1(I))ds \\ &+ \xi_1\xi_2 \int_{outside(\Gamma)} (\ln \pounds_2(I))ds \\ &+ \xi_1\xi_2 \int_{inside(\Gamma)} (\ln \pounds_3(I'))ds \\ &+ \xi_1\xi_2 \int_{outside(\Gamma)} (\ln \pounds_4(I'))ds, \end{aligned} \tag{3. 1}$$

where,

$$\pounds_1 = \frac{-1}{\sqrt{2\pi}\varsigma_1}\exp\Big(\frac{(I(\alpha,\beta)-\zeta_1)^2}{2\varsigma_1^2}\Big), \quad \pounds_2 = \frac{-1}{\sqrt{2\pi}\varsigma_2}\exp\Big(\frac{(I(\alpha,\beta)-\zeta_2)^2}{2\varsigma_2^2}\Big),$$

$$\pounds_3 = \frac{-1}{\sqrt{2\pi}\varsigma_3}\exp\Big(\frac{(I'(\alpha,\beta)-\chi_1)^2}{2\varsigma_3^2}\Big), \quad \pounds_4 = \frac{-1}{\sqrt{2\pi}\varsigma_4}\exp\Big(\frac{(I'(\alpha,\beta)-\chi_2)^2}{2\varsigma_4^2}\Big),$$

and ζ_1, ζ_2 are the averages of given image inside and outside respectively and d_1, d_2 are the averages of difference image inside and outside respectively and ς_i^2, where $i = 1,2,3,4$ denotes the corresponding variances.

In detail, local chan-vese model only takes global image statistics. In segmentation of inhomogeneous noisy images local chan-vese model causes weak detection of boundaries, because local chan-vese model only uses global image statistics. Therefore, model (3.1) is introduced which is a new image segmentation model. The proposed model (3.1) uses both local and global statistics. Therefore, the proposed model (3.1) works more good and efficiently in segmenting the homogenous and in-homogenous noisy images. Moreover, the local statistics of image helps in capturing a local minute details and ignoring the noise while global image statistics provides robust, fast detection of global image structure and provide a good result in noisy images.

Now we minimizing the energy functional given in Eq. (3.1). For a fixed level set function ψ, we minimize the energy functional in Eq. (3.1) with respect to ζ_1, ζ_2, χ_1, χ_2 and variances . Using variational calculus, we can prove that the constant functions ζ_1, ζ_2, χ_1, χ_2 and variances that reduce the energy functional in Eq. (3.1) for a fixed function ψ as given below:

$$\zeta_1(\psi) = \frac{\int_\Omega I(\alpha,\beta)\mathcal{H}(\psi)d\alpha d\beta}{\int_\Omega \mathcal{H}(\psi)d\alpha d\beta}, \quad \zeta_2(\psi) = \frac{\int_\Omega I(\alpha,\beta)(1-\mathcal{H}(\psi))d\alpha d\beta}{\int_\Omega (1-\mathcal{H}(\psi))d\alpha d\beta},$$

$$\chi_1(\psi) = \frac{\int_\Omega I'(\alpha,\beta)\mathcal{H}(\psi)d\alpha d\beta}{\int_\Omega \mathcal{H}(\psi)d\alpha d\beta}, \quad \chi_2(\psi) = \frac{\int_\Omega I'(\alpha,\beta)(1-\mathcal{H}(\psi))d\alpha d\beta}{\int_\Omega (1-\mathcal{H}(\psi))d\alpha d\beta}.$$

And

$$\varsigma_1^2(\psi) = \frac{\int_\Omega (I(\alpha,\beta)-\zeta_1)^2\mathcal{H}(\psi)d\alpha d\beta}{\int_\Omega \mathcal{H}(\psi)d\alpha d\beta}, \quad \varsigma_2^2(\psi) = \frac{\int_\Omega (I(\alpha,\beta)-\zeta_2)^2(1-\mathcal{H}(\psi))d\alpha d\beta}{\int_\Omega (1-\mathcal{H}(\psi))d\alpha d\beta},$$

$$\varsigma_3^2(\psi) = \frac{\int_\Omega (I'(\alpha,\beta)-\chi_1)^2\mathcal{H}(\psi)d\alpha d\beta}{\int_\Omega \mathcal{H}(\psi)d\alpha d\beta}, \quad \varsigma_4^2(\psi) = \frac{\int_\Omega (I'(\alpha,\beta)-\chi_2)^2(1-\mathcal{H}(\psi))d\alpha d\beta}{\int_\Omega (1-\mathcal{H}(\psi))d\alpha d\beta}.$$

Now keeping ζ_1, ζ_2, χ_1, χ_2 and variances fixed, and minimizing the overall energy functional given in Eq. (3.1) with respect to ψ. We did the minimization of Eq. (3.1) by involving a time artificial variable $t \geq 0$, hence minimization of energy functional given in Eq. (3.1) for fixed ζ_1, ζ_2, χ_1, χ_2 and variances is given by:

$$\begin{aligned} \psi_t = \frac{\partial\psi}{\partial t} &= \xi_1\xi_2\Big[\ln\frac{\varsigma_2^2}{\varsigma_1^2} + \frac{(I(\alpha,\beta)-\zeta_1)^2}{\varsigma_1^2} - \frac{(I(\alpha,\beta)-\zeta_2)^2}{\varsigma_2^2}\Big] \\ &+ \xi_1\xi_2\Big[\ln\frac{\varsigma_4^2}{\varsigma_3^2} + \frac{(I'(\alpha,\beta)-\chi_1)^2}{\varsigma_3^2} - \frac{(I'(\alpha,\beta)-\chi_2)^2}{\varsigma_4^2}\Big]. \end{aligned}$$

The following section of this monograph, shows the applicability of the above new research work. In precise way we can say that the coming section shows the numerical work regarding the energy functional of our new proposed model.

4. Experimental Results:

This section contains some experimental results of LCV model and proposed model. These experimental results shows the efficiency and better performance of our new proposed model, as compared to LCV model regarding noisy images. Initial contour can be considered any where on the original noisy image. We present three set of images for each model, i.e. original image, final contour and the segmented result. The comparison for each image is elaborated in the corresponding remark.

Experimental result of LCV model

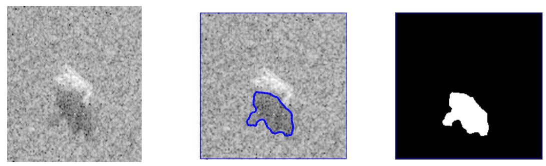

(a) Original Image (b) LCV Result (c) Final Result

FIGURE 1. The figure illustrating the performance of LCV model. (a) Original synthetic Image (b) LCV model Result (c) Final Result.

Experimental result of proposed model

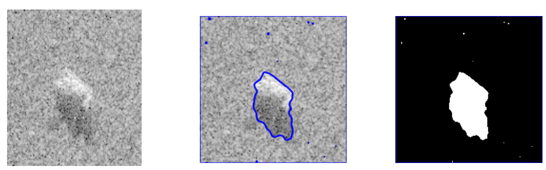

(a) Original Image (b) proposed Result (c) Final Result

FIGURE 2. The figure illustrating the performance our proposed SEGMENTATION model. (a) Original synthetic Image (b) proposed model Result (c) Final Result.

Remark 4.1. *The above figure is an original satellite image. The result of figures 3 and 4 shows the robustness of LCV and proposed models, respectively. Clearly, the result of proposed model is more efficient as compared to LCV model, because proposed model captured more information of the original image.*

Experimental result of LCV model

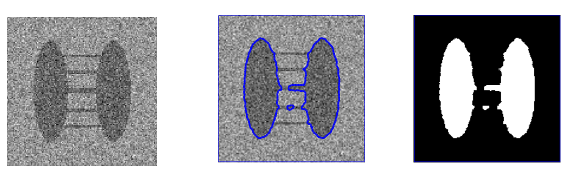

(a) Original Image (b) LCV Result (c) Final Result

FIGURE 3. The figure illustrating the performance of LCV model. (a) Original synthetic Image (b) LCV model Result (c) Final Result.

Experimental result of proposed model

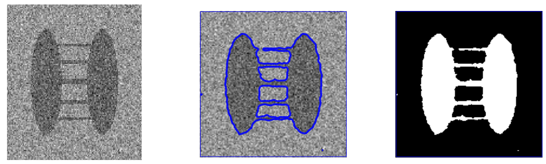

(a) Original Image (b) proposed Result (c) Final Result

FIGURE 4. The figure illustrating the performance of our new proposed SEGMENTATION model. (a) Original synthetic Image (b) proposed model Result (c) Final Result.

Remark 4.2. *The above figure is an original satellite image. The result of figures 1 and 2 shows the robustness of LCV and proposed models, respectively. Clearly, the proposed model Result is more efficient as compared to LCV model, because proposed model captured more information of the original image.*

Experimental result of LCV model

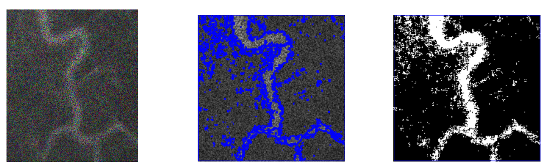

(a) Original Image (b) LCV Result (c) Final Result

FIGURE 5. The figure illustrating the performance LCV model. (a) Original Image (b) LCV model Result (c) Final Result.

Experimental result of proposed model

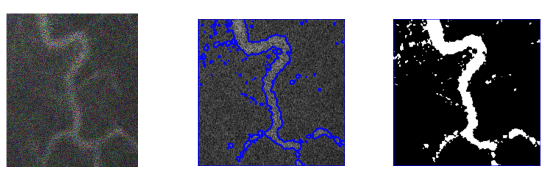

(a) Original Image (b) proposed Result (c) Final Result

FIGURE 6. The figure illustrating the performance our proposed SEGMENTATION model. (a) Original Image (b) proposed model Result (c) Final Result.

Remark 4.3. *The above figure is a real medical noisy image. The result of figures 7 and 8 shows the robustness of LCV and proposed models, respectively. Clearly, the result of* *proposed model is more efficient as compared to LCV model, because proposed model captured less noise.*

Experimental result of LCV model

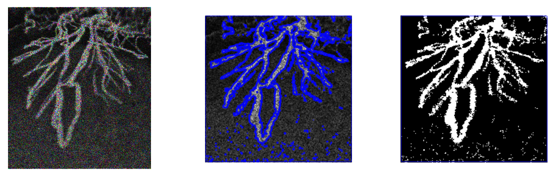

(a) Original Image (b) LCV Result (c) Final Result

FIGURE 7. The figure illustrating the performance of LCV model. (a) Original Image (b) LCV model Result (c) Final Result.

Experimental result of proposed model

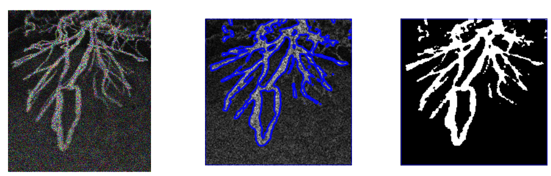

(a) Original Image (b) proposed Result (c) Final Result

FIGURE 8. The figure illustrating the performance our proposed SEGMENTATION model. (a) Original Image (b) proposed model Result (c) Final Result.

Remark 4.4. *The above figure displays a real noisy medical image. The result of figures 5 and 6 shows the robustness of LCV and proposed models, respectively. Clearly, the result of proposed model is more efficient as compared to LCV model, because proposed model captured less noise.*

5. CONCLUSION

In a nutshell we can precisely claim that our new proposed model for noisy intensity inhomogeneity images is actually the amalgam of both LCV model and Noisy image segmentation model. Precisely the new model is less time consuming and probably can be adopted instead of traditional level set methods by introducing a new penalizing energy to the regularization term. Specially, the evolving curve in level set evolution process can automatically stop on true boundaries of objects. Furthermore, the new model is also based on logarithmic function and it is founded on the basis of nonlinear diffusion model [7]. The new model gives us better results as compared to the traditional models which we witnessed in the above experimental works.

6. Acknowledgments

I am grateful to the reviewers for their comments which further flourish the quality of this paper. In addition, I am also grateful to Mr. Gulzar Ali lecturer at Karnal Sher Khan Cadet College Swabi, Pakistan who edited my grammatical mistakes as well as imparted me certain useful tips for research writing.

7. Authors' Contributions

Both the authors Sartaj Ali and Beenesh Dayyan contributed equally and significantly in writing this paper. They also read and approved the final manuscript.

References

[1] S. E. Ahmed, *A Pooling Methodology For Coefficient Of Variation*, Sankhya: The Indian Journal of Statistics **57**, (1995) 57–75.

[2] R. Adams and L. Bischof, *Seeded region growing*, IEEE Trans. Pattern Analysis and Machine Intelligence **16**, (1994) 641-647.

[3] T. M. Al-Shami, *Somewhere Dense sets and ST_1-spaces*, Punjab Univ. j. math. **49**, No. 2 (2017) 101-111.

[4] N. Badshah and K. Chen, *Image Selective Segmentation under Geometrical Constraints Using an Active Contour Approach*, Math. Comp. **7**, (2010) 759–778.

[5] V. Caselles, R. Kimmel and G. Sapiro, *Geodesic Active Contours*, International Journal of Computer Vision **22**, (1997) 61–79.

[6] T. F. Chan and L. A. Vese, *Active contours without edges*, IEEE Transactions on Image Processing **10**, (2001) 266–277.

[7] B. Chen, Y. Li and J. L. Cai, *Noisy image segmentation based on nonlinear diffusion equation model*, Elsevier, Applied Mathematical Modelling, **36**, (2012) 1197–1208.

[8] K. Chen, *Matrix Preconditioning Techniques and Applications*, Cambridge University Press, The Edinburgh Building, Cambridge UK, first edition, 2005.

[9] C. Gout, C. L. Guyader and L. A. Vese, *Segmentation under geometrical conditions with geodesic active contour and interpolation using level set method*, Numerical Algorithms **39**, (2005) 155–173.

[10] C. L. Guyader and C. Gout, *Geodesic active contour under geometrical conditions theory and 3D applications*, Numerical Algorithms **48**, (2008) 105–133.

[11] M. Jeon, M. Alexander, W. Pedrycz and N. Pizzi, *Unsupervised hierarchical image segmentation with level set and additive operator splitting*, PRL. **26**, (2005) 1461–1469.

[12] M. Kass, A. Witkin and D. Terzopoulos, *Active Contours Models*, International Jornal of Computer Vision (1988) 321–331.

[13] Y. Leclerc, *Region growing using the MDL principle*, In: DAPPRA Image Understanding Workshop, 1990.

[14] T. Lu, P. Neittaanmaki and X. C. Tai, *A parallel splitting up method and its application to Navier-Stokes equations*, Appl. Math. Lett. **4**, (1991) 25–29.

[15] L. Modica and S. Mortola, *Un esempio di Un Γ-convergenza*, *Boll. Un. Mat. Ital.* **14**, (1997) 285–299.

[16] M. Mora, C. Tauber and H. Batatia,*Robust Level Set for Heart Cavities Detection in Ultrasound Images*, Computers in Cardiology **32**, (2005) 235–238.

[17] D. Mumford and J. Shah. *Optimal approximation by piecewise smooth functions and associated variational problems*, Communications on Pure Applied Mathematics **42**, (1989) 577–685.

[18] S. Osher and R. Fedkiw, Γ-*Level Set Methods and Dynamic Implicit Surfaces*, springer verlag, 2003 Lec. Notes Comp. Sci. **3708**, (2005) 499–506.

[19] S. Osher and J. A. Sethian, *Fronts propagating with curvature-dependent speed: algorithms based on Hamilton-Jacobi formulations*, J. Comput. Phys. **79**, (1988) 12–49.

[20] M. Sivasubramanian, *A Brief Review of Kalimuthu's Geometrical Publications*, Punjab Univ. j. math. **49**, No. 2 (2017) 153-159.

[21] M. A. Schulze and Q. X. Wu, *Nonlinear Edge-Preserving Smoothing of synthetic Aperture Radar Images*, Proceedings of the New Zealand Image and Vision Computing 95 Workshop (1995) 65–70.

[22] J. A. Sethian, *Level Set Methods and Fast Marching Methods*, Evolving interfaces in Computational Geometry, Fluid Mechanics, Computer Vision and Material Science, Cambridge University Press, Londres, 1999.

[23] L. A. Vese and T. F. Chan, *A multiphase level set framework for image segmentation using the Mumford and Shah model*, Int. J. Computer Vision, **50**, (2002) 271–293.

[24] L. Vincent and Soille, *Watersheds in Digital Spaces - an efficient algorithm based on immersion*, IEEE Trans. Pattern Analysis and Machine Learning **6**, (1994) 583–598.

[25] J. Weickert, B. M. ter Haar Romeny and M. A. Viergever, *Efficient and reliable schemes for nonlinear diffusion filtering*, IEEE Trans. Image Proc. **7**, (1998) 398–410.

[26] J. Weickert and G. Kuhne, *Fast methods for implicit active contours models*. In: Geometric Level SetMethods in Imaging, Vision, and Graphics, (2003) 43–58.